Reference heat capacity for asteroid regolith from 10 to 1000K.

J. Biele[1], M. Grott[2], [1]German Aerospace Center DLR RB-MSC, Linder Höhe 1, 51147 Köln, Germany, jens.biele@dlr.de, [2]German Aerospace Center DLR-PF, Rutherfordstr. 2, 12489 Berlin, Germany, matthias.grott@dlr.de

Introduction: Remote sensing in the mid-infrared allows the estimation of the thermal effusivity or thermal inertia $\Gamma=(\rho k(T)c_p(T))^{1/2}$ of the surface material, with T absolute temperature, k thermal conductivity, ρ bulk density, and c_p heat capacity at constant pressure in units of J/kgK. Knowledge or an estimate of $c_p(T)$ is required to extract, e.g., $k(T)$, which in turn allows estimation of grain sizes by applying models of heat transport in porous media [1-2].

While the temperature dependence of c_p is a second-order effect at room temperature and does not strongly dependent on the chosen material (besides the mass fraction of metallic FeNi), c_p shows very strong temperature and composition dependence at low temperatures. Heat capacity goes to zero as T approaches zero, and it is proportional to T^3 at very low temperatures. It shows a slight linear increase as T approaches large values due to the difference $c_p - c_v$, as only c_v obeys the 3R/atom Dulong-Petit limit.

Method and results: Using measured lunar [3-4] and meteorite data for ordinary H and L chondrites as well as mineral heat capacities and known lunar and meteorite compositions [5-6], we construct a new reference model curve for the isobaric heat capacity c_p of small body surface material over a wide temperature range. The model is applicable from 10 to 1000 K and stays physical from 0 K to the melting temperature of silicates (~1400 K). The model includes terms describing the dependence of c_p on the mass fraction of meteoritic iron (FeNi) and the mass fraction of organic materials; an extension to low temperature regolith with a composition dominated by ices and tholins is planned.

Lunar Regolith: A new convenient rational log-log fit function for the reference lunar average $c_p(T)$ is given by

$$\ln\left(\frac{c_{p,lunar}(T)}{1J/kg/K}\right)=\frac{p_1x^3+p_2x^2+p_3x+p_4}{x^2+q_1x+q_2}$$

$$x=\ln(T/1K)$$

and the fit parameters are given by

$p_1 = 3$, $p_2 = -54.4484$, $p_3 = 306.8465$, $p_4 = -376.5795$, $q_1 = -16.8077$, and $q_2 = 87.3213$.

This rational function has no poles and correctly predicts zero heat capacity at 0 K and a ~T^3 dependence at T < 5 K. It fits the lunar sample data with an absolute maxium deviation of 3%, the high temperature model to better than 1% . The uncertainty of the low temperature portion rapidly increases below 50 K to ~5-10%.

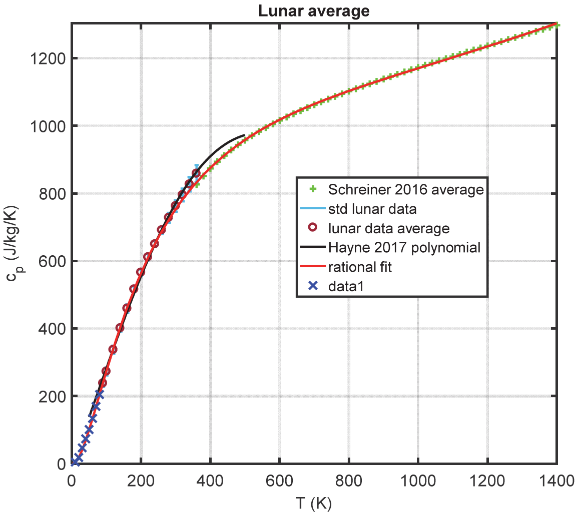

Figure 1: Lunar cp reference curve from 0 to 1400K compared to lunar sample data points and earlier fits [4,6]. Average over mare and highland data and compositions. Native FeNi content ~0.3%

FeNi Content: The main compositional dependence is on the native metal (meteoritic iron) content. Since c_p of FeNi is much smaller than that of silicates, meteorites or regolith containing FeNi have a lower c_p. If w is the mass fraction of meteoritic iron in the material, heat capacity of the mixture can be expressed as

$$c_p = c_{p,FeNi}w + c_{p,Silicates}(1-w)$$

The heat capacity of both iron and nickel has a number of magnetic and structural transitions, thus steps and lambda-peaks in the c_p(T) curves at temperatures >600K exist. Fe-Ni alloys show a complicated dependence of the transition temperatures and amplitudes on composition and the measured c_p-curve for a typical Ni content of 10% is chosen for high temperatures. At lower Ni contents, an ideal mixture is assumed [7-9].

It appears likely that for experimental methods like remote sensing, which average large quantities of regolith of varying composition (also in alloys and solid solutions), the sharp steps and transition peaks are smoothed out.

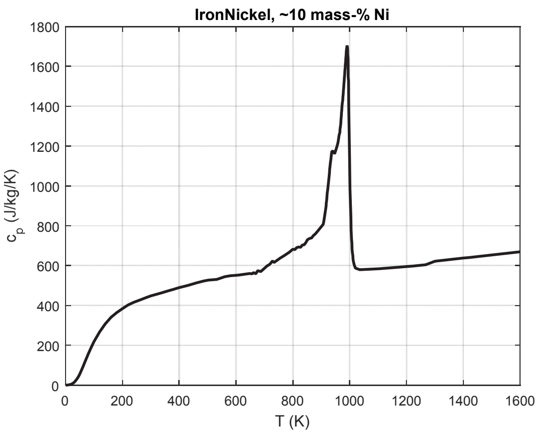

Figure 2: Composite cp for 10% Ni (by mass). Numerical data suitable for interpolation can be obtained from the authors upon request.

Carbon Content: It is known that the heat capacity of ordinary and carbonaceous chondrites is similar [10]. It is interesting to note that the c_p of graphite is higher than that of silicate minerals and that the heat capacity of bituminous coal (dry, ash-free) is even ~50% higher than that of graphite due to organic volatiles which completely decompose to graphite at ~1300K. Thus carbonaceous chondrites should have a higher heat capacity than low-metal chondrites or lunar regolith. We fit the available c_p data for graphite [11,12] over the temperature range 0-3000 K using

$$c_{p,graphite} = \left(1+\beta T\right) \Big/ \left[A T^{n_1} + B T^{n_2} \right] \quad \text{J/kg/K}$$

A = 33.71, B = 0.0008027, β= -2.872e-5, n_1 = -1.852
n_2 = -0.08413 , rmse= 2.2 J/kg/K,

The c_p of typical bituminous coal with a total volatile matter content of 30-40% [13,14] can be approximated by

$$\frac{c_{p,coal}}{c_{p,graphit}} \cong 1.562 - 3.732 \cdot 10^{-5} T - 3.283 \cdot 10^{-7} T^2$$

Then, $c_p = c_{p,coal} w + c_{p,oc}(1-w)$ where now w is the mass fraction of carbonaceous matter and $c_{p,oc}$ is the heat capacity of ordinary chondrites.

Conclusion: A database of heat capacity data for a number of common minerals for both low and high temperatures has been collected from a critical evaluation of the literature including heat capacity data of meteorites. The new c_p-equation for lunar materials is physical over a wide temperature range and can be extended to any composition. A simple composition dependent model for mass fraction w_1 of FeNi and mass fraction w_2 of organics/carbon is given by

$$c_p(T) = w_1 c_{p,FeNi}(T) + w_2 c_{p,coal}(T) + (1 - w_1 - w_2) c_{p,\text{lunar}}(T)$$

It is worth noting that if Γ is the observable, the product of density ρ and heat capacity c_p usually is the quantity of interest. As silicates, coal, and FeNi have very different densities of 3000, 1350 and 8000 kg/m³, respectively, the same mass fraction of FeNi has a much larger impact on Γ than carbon.

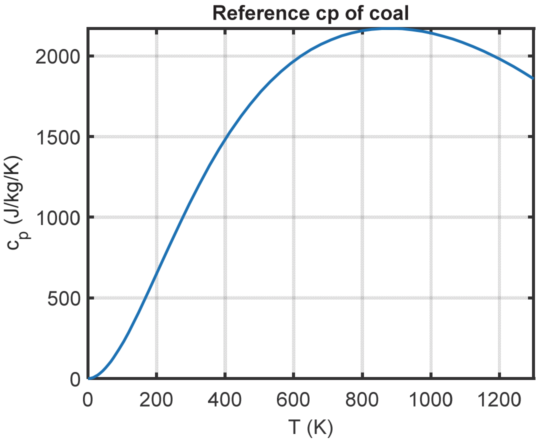

Figure 3: Reference cp of coal as a function of temperature.

References: [1] Gundlach, B. and J. Blum (2013), *Icarus* **223**(1): 479-492. [2] Sakatani, N., et al. (2017, *AIP Advances* **7**(1): 015310. [3] Robie, R. A., B. S. Hemingway and W. H. Wilson (1970), Science 167(3918):749-750. [4] Hemingway, B. S., et al. (1973) *LPSC Proceedings*. Vol. 4. [5] Schreiner, S. S., et al. (2016), Adv. Space Res. 57(5): 1209-1222. [6] Hayne, P. O., et al. (2017), JGR Planets, online 4 December 2017. [7] Meschter, P. J., et al. (1981). Journal of Physics and Chemistry of Solids **42**(9): 861-871. [8] White, G. K. and M. L. Minges (1997). , International Journal of Thermophysics **18**(5): 1269-1327. [9] Wilthan, B. (2002). Thesis, TU Graz. [10] Consolmagno, G. J., et al. (2013). PSS **87**: 146-156 [11] Burchell, T. D. (2012). Graphite. In: Comprehensive Nuclear Materials: R. J. M. Konigs. Amsterdam, Elsevier. **2:** 285–305. [12] DeSorbo, W. and W. Tyler (1953), The Journal of Chemical Physics **21**(10): 1660-1663. [13] Leśniak, B., et al. (2013), Chemik **67**: 560-571 [14] Richardson, M. J. (1993), Fuel **72**(7): 1047-1053